Phononic Coupled-Resonator Waveguide Micro-Cavities

Ting-Ting Wang [1,2] , **Sylwester Bargiel** [2] , **Franck Lardet-Vieudrin** [2], **Yan-Feng Wang** [3] ,
Yue-Sheng Wang [1,3] **and Vincent Laude** [2,*]

[1] Institute of Engineering Mechanics, Beijing Jiaotong University, Beijing 100044, China;
    tingting_wang1992@163.com (T.-T.W.); yswang@tju.edu.cn (Y.-S.W.)
[2] Institut FEMTO-ST, CNRS UMR 6174, Université Bourgogne Franche-Comté, 25030 Besançon, France;
    sylwester.bargiel@femto-st.fr (S.B.); franck.lardet@femto-st.fr (F.L.-V.)
[3] School of Mechanical Engineering, Tianjin University, Tianjin 300350, China; wangyanfeng@tju.edu.cn
[*] Correspondence: vincent.laude@femto-st.fr

Featured Application: Engineered phononic resonances in the ultrasonic range.

Abstract: Phononic coupled-resonator waveguide cavities are formed by a finite chain of defects in a complete bandgap phononic crystal slab. The sample is machined in a fused silica plate by femtosecond printing to form an array of cross-shape holes. The collective resonance of the phononic cavities, in the Megahertz frequency range, are excited by a piezoelectric vibrator and imaged by laser Doppler vibrometry. It is found that well-defined resonant cavity modes can be efficiently excited, even though the phononic cavities are distant by a few lattice spacings and are only weakly coupled through evanescent elastic waves. The results suggest the possibility of engineering the dynamical response of a set of coupled phononic cavities by an adequate layout of defects in a phononic crystal slab.

Keywords: phononic crystal; phononic cavity; evanescent coupling

---

1. Introduction

The engineering of phononic resonances enables the excitation of localized vibrations of microscopic objects at ultrasonic frequencies, forming meta-atoms or meta-molecules with precise eigenfrequencies and elastic waveforms. They have potential applications as sensor elements [1], MEMS resonators [2], elastic waveguides [3], or optomechanical systems [4–7], for instance.

Phononic resonances are naturally induced at the microscale with three-dimensional mechanical structures attached to a surface, for instance, in the form of erected pillars [8] or chains of resonators [3,9]. One requirement is that clamping to the surface or support does not reduce too significantly the quality factor of resonances through radiation of outgoing elastic waves. Another approach that is prone to engineering relies on phononic crystals [10–12]. One of their important features is indeed the formation of complete band gaps, inside which wave propagation is forbidden and only evanescent waves can exist.

By introducing defects in a phononic crystal, spatially-localized states are introduced with precise resonant frequencies. Further forming an infinite chain of such defects leads to the concept of the coupled-resonator elastic waveguide (CREW) [13], originally inspired by coupled-resonator optical waveguides in photonic crystals (CROW) [14]. It is known that the dispersion of waves guided along a CREW is very smooth and is determined by the coupling coefficients existing between phononic resonators. When the chain is made finite, a discrete set of resonance frequencies established along the dispersion relation for guided waves; we hence term the chain a coupled-resonator waveguide cavity.

The resonant states are collective vibrations of the chain, as we have shown recently in the case of a chain of seventeen resonators implemented in a two-dimensional fused silica phononic crystal slab, and are rather independent of the path followed over the surface of the slab [15].

In this paper, we experimentally explore how a set of a few phononic coupled-resonator waveguide cavities, coupled weakly through evanescent elastic waves, can form collective vibrations where the resonance modes of the individual phononic cavities are essentially preserved but can be excited at once. Experimentally, we rely on the phononic crystal slab technology developed for our previous work based on femtosecond laser writing followed by KOH etching of a fused silica plate [15], but extend our considerations to the set of three short phononic cavities shown in Figure 1. In the following, we first present the experimental results and the numerical simulations that sustain them, before discussing the observed collective vibrations in the light of a dynamical matrix model with one degree of freedom per defect and the nearest-neighbor approximation.
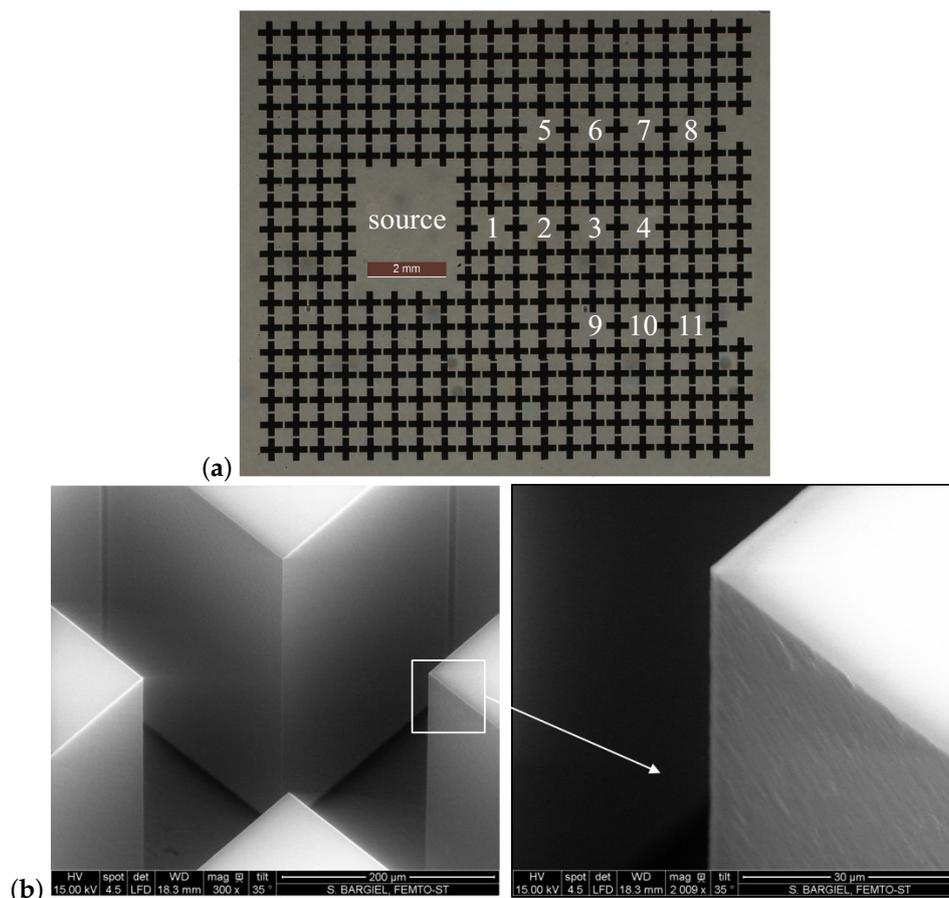

Figure 1. (**a**) Optical microscope image of the sample considered in this work. The 500 μm-thick fused silica plate is processed by femtosecond laser-assisted wet etching (FLAE). Cross-holes are removed from the plate to define a phononic crystal slab structure with 18 rows and 20 columns. Defects, numbered from 1 to 11, define a set of three coupled-resonator waveguide cavities. The source region, placed inside the crystal structure, is in contact from the bottom with a piezoelectric vibrator. Out-of-plane displacements of the top surface are measured by a scanning laser vibrometer. The lattice spacing is $a = 714$ μm. (**b**) Scanning electron microscope view of a cross-hole and zoomed view at a corner showing the side-wall rugosity.

2. Results

The phononic crystal slab sample we consider is shown in Figure 1. The crystal itself is a square lattice of cross-holes [16] with lattice constant $a = 714$ μm. Between each group of four nearest holes, a square-shape membrane resonator is defined and is connected to its four neighbors.

The phononic crystal slab has a large complete bandgap that is detailed later on. As a note, cross-holes provide a much wider bandgap width than circular holes, for instance [16]. There are even other unit-cell designs that still allow gaining on the bandgap width [17], but we selected cross-holes in this work because of the simpler footprint for technology. For frequencies within the complete bandgap, there are only evanescent Bloch waves and the coupling between defects decreases exponentially with their separation. A total of eleven identical defects are introduced and are grouped in three coupled-resonator waveguide cavities: defects 1–4 form CREW cavity C1, defects 5–8 form CREW cavity C2, and defects 9–11 form CREW cavity C3. Defect resonators in the cavities are separated by a distance $2a$. Comparatively, the shortest distance between two cavities is $4a$. Hence, it is expected that CREW cavities are only weakly coupled. Experimental details regarding sample preparation and characterization are identical with Ref. [15] and are not repeated here.

The phononic crystal dispersion properties are summarized in Figure 2. All computations are performed using the finite element method. Phononic band structures are obtained using the unit-cell of Figure 2a for the phononic crystal and using the unit-cell of Figure 2b for the CREW. Periodic boundary conditions are applied on all lateral sides, whereas the bottom and top surfaces are left free; the Bloch wavevector is fixed and frequencies are obtained by solving an eigenvalue problem [13]. The band structures are shown only for out-of-plane polarized Bloch waves, as only that displacement component is accessible in our experiments. Geometrical parameters are chosen to ensure the existence of a wide complete bandgap, extending between 1.7 and 4 MHz except from a flat bulk band appearing around 3.2 MHz. The smallest length in the structure is $a - b = a/10 = 71$ μm, much larger than the estimated resolution of ≈ 1 μm of the technological process for the holes. The CREW considered in this paper are formed from defects separated by two lattice constants. Defects are simply created by omitting to etch chosen cross holes. As a result, it is expected that elastic waves can become spatially localized around the defects, for frequencies inside the complete bandgap, decaying exponentially away from the defect center [18–20]. If defects are placed not too far away from one another, they are in their mutual near-fields and are thus evanescently coupled. Guided elastic waves can then transit from one defect to the next. The dispersion of guided waves in a CREW is very smooth and is dictated by the coupling coefficients between resonant defects [13]. In Figure 2, many guided bands appear within the complete bandgap, each of them originating from a given resonant mode. In relation to experiments, we have selected three frequency ranges around 2.25 MHz (range A), 3 MHz (range B), and 3.55 MHz (range C). A total of five guided waves are apparent, each with their specific modal shape. The two pairs of guided waves in ranges A and C have orthogonal polarizations and hence their dispersion curves can cross without interference. Their respective actual excitations in the experiment depend on the symmetry of the excitation source.

Ultrasonic waves in the experimental sample of Figure 1 are excited thanks to a piezoelectric vibrator in contact with the bottom surface in the source region. Coupling from the source region to the resonators occurs mainly with defect 1. Out-of-plane vibrations at the top surface are measured using a scanning laser vibrometer (Polytec Microsystem Analyzer MSA-500, equipped with analog displacement decoder model DD-300; 0.03-24 MHz frequency response with 50 nm/V sensitivity). The source waveform sent to the piezoelectric vibrator is a periodic chirp covering the frequency range of interest. The amplitude of out-of-plane displacement measured at three different locations is plotted in Figure 3a. Measurements averaged over defect 4 are considered typical of CREW cavity C1, whereas measurements for CREW cavities C2 and C3 are averaged over the unit cells just right of defect 8 and defect 11, respectively. Displacements larger than 0.3 pm can be recorded with this setting. The measurements reveal a sequence of very sharp resonance peaks, in agreement with previous results on a sample with a single chain of seventeen coupled resonators [15]. Compared with that sample, however, the resonance peaks are distributed over a larger span of frequencies, especially in the range from 2.1 to 2.3 MHz.
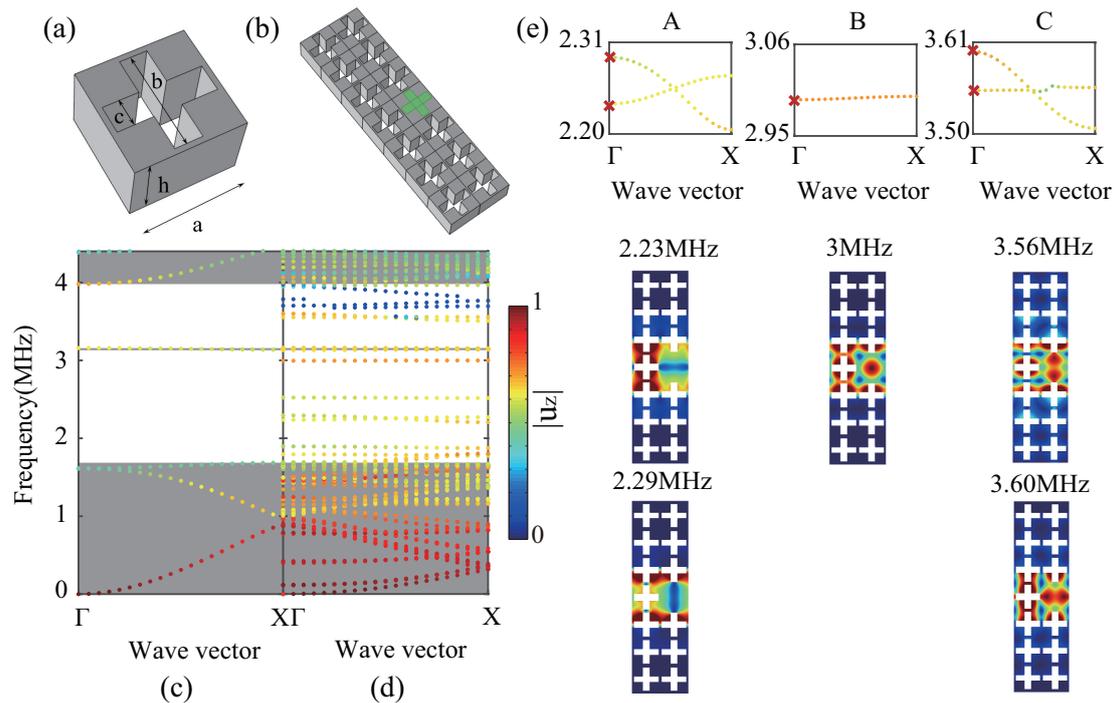
Figure 2. Dispersion of the phononic crystal slab of cross holes. (**a**) The primitive unit cell is defined by four parameters: the lattice constant a, the slab thickness h, the cross length b, and the cross width c. (**b**) A coupled-resonator elastic waveguide (CREW) is formed from defects separated by two lattice constants and created by omitting one hole. The depicted supercell has seven rows and two columns. (**c**) The band structure of the crystal is shown for out-of-plane modes only and for $b/a = 0.9$, $c/a = 0.25$, and $h/a = 0.7$. The complete bandgap appears between the gray regions. The color scale of the bands is proportional to the out-of-plane component of displacement. (**d**) The band structure of the CREW contains a series of flat (small dispersion) bands, each holding a guided Bloch wave. (**e**) Close-up views of three selected frequency ranges are shown. Eigenmodes at the Γ point of the first Brillouin zone are shown for each of the five bands.

Measurements can be compared directly with a finite element model based on a stochastic force distribution applied in the source region [21]. To this end, a three-dimensional mesh is created to represent the full sample shown in Figure 1, with a perfectly matched layer (PML) surrounding the finite size crystal. Free boundary conditions are still applied on the bottom and top surfaces. Material losses in fused silica are added to the model. A fair correspondence is observed between experiment and numerical simulation in Figure 3. In particular, the distribution of resonance peaks and their central frequencies are rather well-reproduced numerically, but the response levels are less reliable. Compared to the experiment, indeed, a fully spatially random body force distribution is considered numerically, whereas the actual piezoelectric excitation has a more symmetrical and homogeneous distribution. Furthermore, the resonance peaks are very narrow and are resolved experimentally with only a few sampling points.

In addition to the frequency response functions shown in Figure 3a, the scanning laser vibrometer can form images of the spatial distribution of the out-of-plane displacement at the surface of the sample at a fixed frequency. We show in Figure 4 the measured displacement fields at three selected frequencies for which maxima of vibration are observed experimentally in CREW cavity C1. Each of these measurements is compared with the finite element numerical simulation obtained at the same frequency.
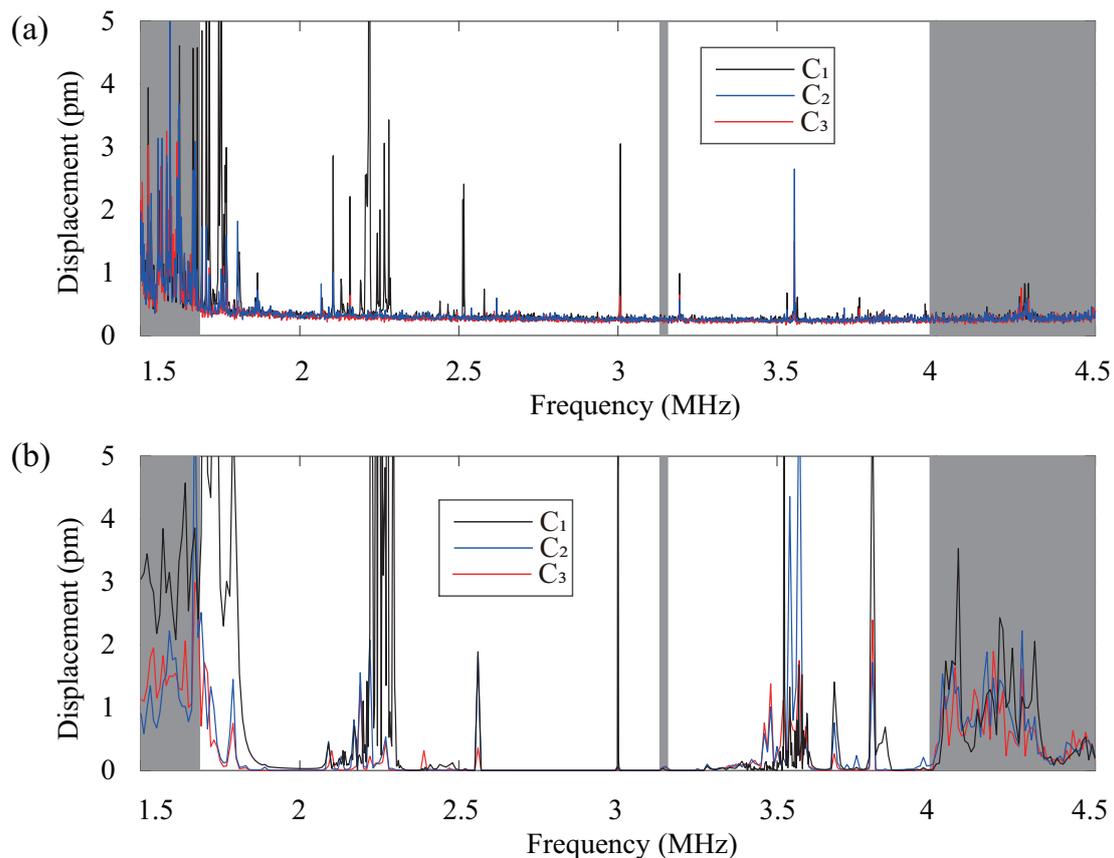
Figure 3. (**a**) Experimental and (**b**) numerical absolute vertical displacement at the position of the received resonators.

At the frequency of 2.26 MHz, vibrations in CREW cavity C1 are clearly excited and the modal shape of the symmetrical mode in range A of Figure 2e is recognized. Comparatively, the antisymmetrical mode in range A is not observed experimentally. The numerical simulation in contrast involves both symmetrical and antisymmetrical modes. As mentioned before, this fact can be explained by the symmetry of the actual source compared to the absence of symmetry of the numerical (random) source.

At the frequency of 3 MHz, the observations are similar for CREW cavity C1 and the modal shape of the non-degenerated mode in range B of Figure 2e is recognized. Faint vibrations in both CREW cavities C2 and C3 are observed as well, with exactly the same modal shape.

At the frequency of 3.56 MHz, the observations are similar again and the modal shape of the symmetrical mode in range C of Figure 2e is recognized in the experimental image. As for 2.26 MHz, the numerical simulation involves both symmetrical and antisymmetrical modes. Clear vibrations in both CREW cavities C2 and C3 are observed at 3.56 MHz, with exactly the same modal shape. There is hence energy transfer from the vibrations of CREW cavity C1 to both CREW cavities C2 and C3, without a significant change in modal shapes, as can be expected in the case of weak coupling of resonant cavities.
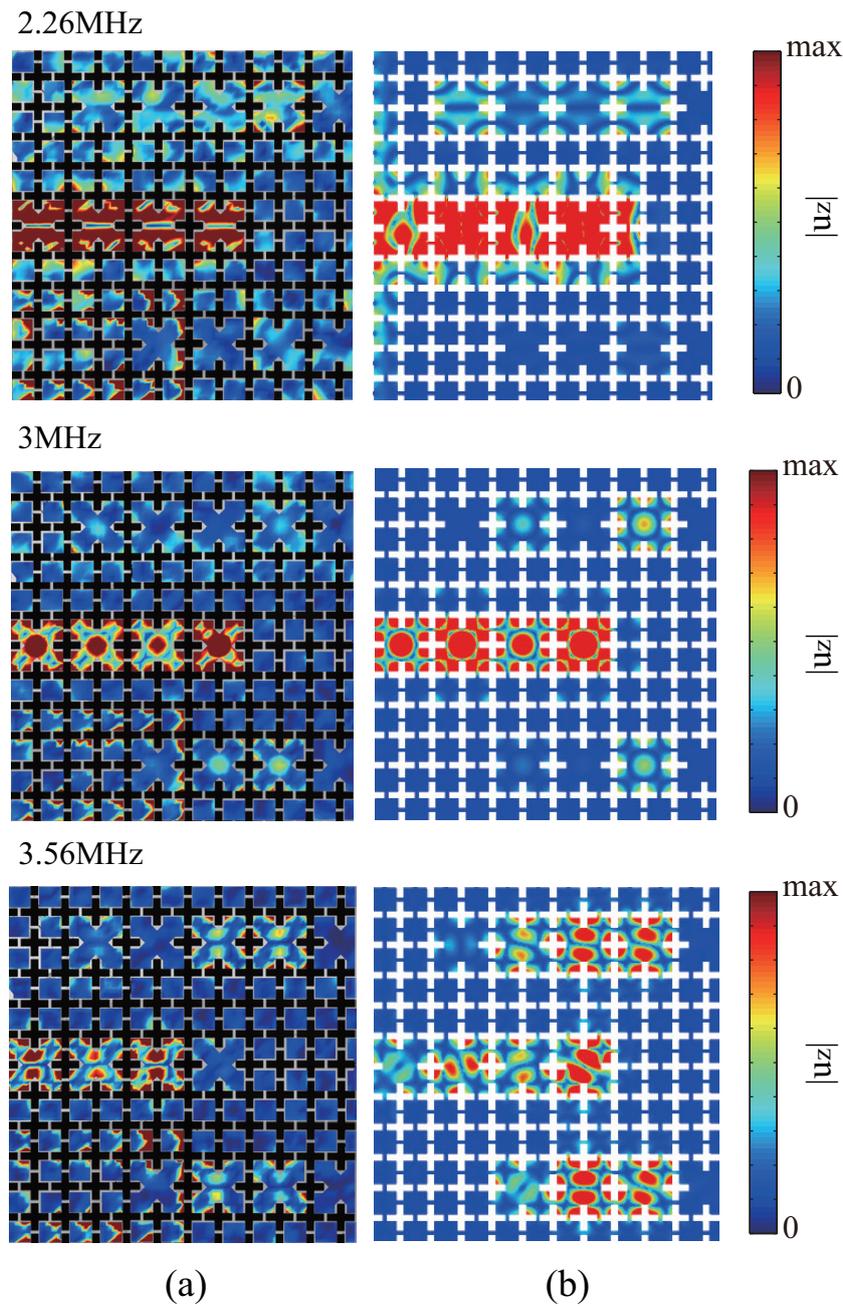
2.26MHz

3MHz

3.56MHz

(a)   (b)

Figure 4. Experimental (**a**) and numerical (**b**) out-of-plane displacement maps at frequencies 2.26 MHz, 3 MHz, and 3.56 MHz.

3. Discussion

In Ref. [15], we introduced a dynamical matrix model to predict the resonant frequencies of a phononic polymer, or a generalized chain of coupled resonators that is not necessarily organized along the principal axes of the supporting phononic crystal. Here we extend the model to the more general case of unequal coupling coefficients. In short, the model assumes that the state of the phononic defect structure is described by one macroscopic degree of freedom per resonator, U_n. All resonators are identical except for a spatial shift in the crystal and have the same isolated resonance frequency ω_0. Then, the dynamical equation for coupled resonators is written

$$-\ddot{U}_m = \sum_{n=1}^{N} D(m,n)U_n, \tag{1}$$

with a symmetric dynamical matrix $D(m, n)$ such that $D(m, m) = \omega_0^2$. The eigenvalues of the dynamical matrix give the observable resonant frequencies of the finite structure. Their number equals the number of resonators for a non-degenerate band.

Within each of the three CREW cavities in this paper, the dominant coupling coefficient is between nearest neighbors, with a lattice separation $2a$. For every waveguide band, the coupling coefficient can be estimated from the frequency extent of the dispersion relation. Hence a coupling coefficient γ can be estimated for each band, or each single defect mode. Furthermore, the CREW cavities are separated by a distance of at least $4a$ (vertically, the separation between defects numbers 2 and 5 is $4a$; similarly the vertical separation between defects numbers 3 and 9 is also $4a$). This leads us to define a coupling coefficient δ that is much smaller than γ to describe the evanescent coupling between CREW cavities 1 and 2, and 1 and 3 as well. Neglecting all other coupling coefficients, we thus can write the dynamical matrix as

$$
D = \begin{pmatrix}
\omega_0^2 & \gamma & 0 & 0 & 0 & 0 & 0 & 0 & 0 & 0 & 0 \\
\gamma & \omega_0^2 & \gamma & 0 & \delta & 0 & 0 & 0 & 0 & 0 & 0 \\
0 & \gamma & \omega_0^2 & \gamma & 0 & \delta & 0 & 0 & \delta & 0 & 0 \\
0 & 0 & \gamma & \omega_0^2 & 0 & 0 & \delta & 0 & 0 & \delta & 0 \\
& & & & \omega_0^2 & \gamma & 0 & 0 & & & \\
& & sym. & & \gamma & \omega_0^2 & \gamma & 0 & & 0 & \\
& & & & 0 & \gamma & \omega_0^2 & \gamma & & & \\
& & & & 0 & 0 & \gamma & \omega_0^2 & & & \\
& & & & & & & & \omega_0^2 & \gamma & 0 \\
& sym. & & & & sym. & & & \gamma & \omega_0^2 & \gamma \\
& & & & & & & & 0 & \gamma & \omega_0^2
\end{pmatrix}.
\tag{2}
$$

The three diagonal blocks account for the eigenfrequencies of CREW cavities C1, C2, and C3, in that sequence. The off-diagonal blocks of the first line provide the weak couplings between CREW cavities.

The discrete dynamical model explains most of the features of the experimental observations of the previous section. Resonances are discrete, appear as sharp peaks centered on the eigenfrequencies of the finite structure, and the modal shapes of the original resonances of the isolated defect resonators remain clearly present in the coupled vibration fields. It also implies that a resonator placed far away from the source of vibrations can be rather efficiently excited, by a mechanism of collective vibrations of the whole phononic crystal structure. Here, cavities placed four phononic crystal rows apart are observed to sustain such collective vibrations.

Before closing this paper, we mention an intriguing observation at frequency 2.09 MHz, reported in Figure 5. At that frequency, the phononic band structure of Figure 2 does not indicate the existence of out-of-plane polarized guided Bloch waves for the $2a$-separated CREW. In contrast, both experiment and numerical simulation indicate the existence of vibration peaks around that frequency. Including also in-plane waves, we show in Figure 5a a close-up view of the phononic band structure. Two additional mostly in-plane polarized bands exist around 2.1 MHz, but the modal shape in Figure 5b is not in agreement with the one observed experimentally in Figure 5c and numerically in Figure 5d, which rules out its contribution to the dynamical response. The numerical simulation in Figure 5d suggests that the out-of-plane vibration excited in CREW cavity C1 may be evanescent (its amplitude decays smoothly from left to right). More investigations are necessary to fully understand the origin of the response at frequency 2.09 MHz, but it seems out of the scope of the dynamical model above.
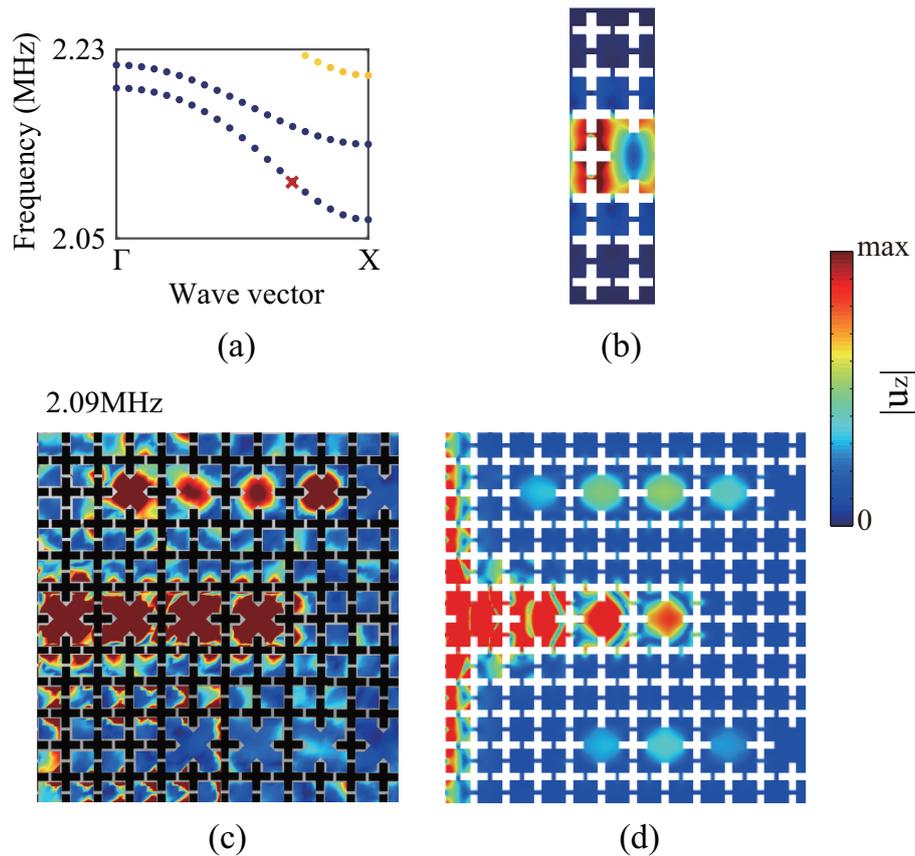
Figure 5. (**a**) Phononic band structure around 2.1 MHz. (**b**) the modal shape at the point marked with a red cross in (**a**) is depicted. Experimental (**c**) and numerical (**d**) out-of-plane displacement maps are shown at frequency 2.09 MHz.

4. Conclusions

As a summary, we have experimentally investigated how a set of three phononic coupled-resonator elastic waveguide cavities form collective vibrations. The CREW cavities are fabricated in a fused silica plate and resonante at a few Megahertz. They are weakly and evanescently coupled for frequencies within the wide complete bandgap, as they are separated by four lattice spacings. Overall, the resonance modes of the individual phononic cavities are essentially preserved and can be excited at once. The observed collective vibrations can generally be explained in the light of a dynamical matrix model with one degree of freedom per defect and within the nearest-neighbor approximation. Beyond this simplified model, the details of the vibrations at resonance are observed by a scanning laser vibrometer. In particular, the vibration modal shapes are found to be consistant with a full finite element model of the experiment.

Author Contributions: conceptualization, T.-T.W. and V.L.; funding acquisition, V.L. and Y.-S.W.; technology, S.B. and T.-T.W.; metrology, F.L.-V. and T.-T.W.; project administration, V.L., Y.-F.W. and Y.-S.W.; software, T.-T.W.; validation, Y.-F.W.; writing—original draft, T.-T.W. and V.L.; writing—review and editing, S.B., F.L.-V., Y.-F.W. and Y.-S.W. All authors have read and agreed to the published version of the manuscript.

Conflicts of Interest: The authors declare no conflict of interest. The funders had no role in the design of the study; in the collection, analyses, or interpretation of data; in the writing of the manuscript, or in the decision to publish the results.

References

1. Lucklum, R.; Li, J. Phononic crystals for liquid sensor applications. *Meas. Sci. Technol.* **2009**, *20*, 124014. [CrossRef]

2. Mahboob, I.; Nishiguchi, K.; Fujiwara, A.; Yamaguchi, H. Phonon Lasing in an Electromechanical Resonator. *Phys. Rev. Lett.* **2013**, *110*, 127202. [CrossRef] [PubMed]

3. Hatanaka, D.; Mahboob, I.; Onomitsu, K.; Yamaguchi, H. Phonon waveguides for electromechanical circuits. *Nature Nanotechnol.* **2014**, *9*, 520. [CrossRef] [PubMed]

4. Gavartin, E.; Braive, R.; Sagnes, I.; Arcizet, O.; Beveratos, A.; Kippenberg, T.J.; Robert-Philip, I. Optomechanical Coupling in a Two-Dimensional Photonic Crystal Defect Cavity. *Phys. Rev. Lett.* **2011**, *106*, 203902. [CrossRef] [PubMed]

5. Safavi-Naeini, A.H.; Hill, J.T.; Meenehan, S.; Chan, J.; Gröblacher, S.; Painter, O. Two-Dimensional Phononic-Photonic Band Gap Optomechanical Crystal Cavity. *Phys. Rev. Lett.* **2014**, *112*, 153603. [CrossRef] [PubMed]

6. Balram, K.C.; Davanço, M.I.; Song, J.D.; Srinivasan, K. Coherent coupling between radiofrequency, optical and acoustic waves in piezo-optomechanical circuits. *Nat. Photon.* **2016**, *10*, 346–352. [CrossRef] [PubMed]

7. Arrangoiz-Arriola, P.; Wollack, E.A.; Pechal, M.; Witmer, J.D.; Hill, J.T.; Safavi-Naeini, A.H. Coupling a superconducting quantum circuit to a phononic crystal defect cavity. *Phys. Rev. X* **2018**, *8*, 031007. [CrossRef]

8. Raguin, L.; Gaiffe, O.; Salut, R.; Cote, J.M.; Soumann, V.; Laude, V.; Khelif, A.; Benchabane, S. Dipole states and coherent interaction in surface-acoustic-wave coupled phononic resonators. *Nat. Commun.* **2019**, *10*, 1–8. [CrossRef] [PubMed]

9. Yamaguchi, H. GaAs-based micro/nanomechanical resonators. *Semicond. Sci. Technol.* **2017**, *32*, 103003. [CrossRef]

10. Wagner, M.R.; Graczykowski, B.; Reparaz, J.S.; El Sachat, A.; Sledzinska, M.; Alzina, F.; Sotomayor Torres, C.M. Two-dimensional phononic crystals: Disorder matters. *Nano Lett.* **2016**, *16*, 5661–5668. [CrossRef] [PubMed]

11. Korovin, A.; Pennec, Y.; Djafari-Rouhani, B. Strong coupling of phononic cavity modes in one-dimensional corrugated nanobeam structures. *Phys. Rev. B* **2017**, *96*, 184302. [CrossRef]

12. Laude, V. *Phononic Crystals: Artificial Crystals for Sonic, Acoustic, and Elastic Waves*, 2nd ed.; De Gruyter: Berlin, Germany, 2020. doi:10.1515/9783110641189. [CrossRef]

13. Escalante, J.M.; Martínez, A.; Laude, V. Dispersion relation of coupled-resonator acoustic waveguides formed by defect cavities in a phononic crystal. *J. Phys. D Appl. Phys.* **2013**, *46*, 475301. [CrossRef]

14. Yariv, A.; Xu, Y.; Lee, R.K.; Scherer, A. Coupled-resonator optical waveguide: a proposal and analysis. *Opt. Lett.* **1999**, *24*, 711. [CrossRef] [PubMed]

15. Wang, T.T.; Bargiel, S.; Lardet-Vieudrin, F.; Wang, Y.F.; Wang, Y.S.; Laude, V. Collective Resonances of a Chain of Coupled Phononic Microresonators. *Phys. Rev. Appl.* **2020**, *13*, 014022. [CrossRef]

16. Wang, Y.F.; Wang, Y.S.; Su, X.X. Large bandgaps of two-dimensional phononic crystals with cross-like holes. *J. Appl. Phys.* **2011**, *110*, 113520. [CrossRef]

17. Jiang, S.; Hu, H.; Laude, V. Ultra-Wide Band Gap in Two-Dimensional Phononic Crystal with Combined Convex and Concave Holes. *Phys. Status Solidi (RRL) Rapid Res. Lett.* **2018**, *12*, 1700317. [CrossRef]

18. Torres, M.; Montero de Espinosa, F.R.; Garcia-Pablos, D.; Garcia, N. Sonic Band Gaps in Finite Elastic Media: Surface States and Localization Phenomena in Linear and Point Defects. *Phys. Rev. Lett.* **1999**, *82*, 3054. [CrossRef]

19. Psarobas, I.E.; Stefanou, N.; Modinos, A. Phononic crystals with planar defects. *Phys. Rev. B* **2000**, *62*, 5536–5540. [CrossRef]

20. Khelif, A.; Choujaa, A.; Djafari-Rouhani, B.; Wilm, M.; Ballandras, S.; Laude, V. Trapping and guiding of acoustic waves by defect modes in a full-band-gap ultrasonic crystal. *Phys. Rev. B* **2003**, *68*, 214301. [CrossRef]

21. Laude, V.; Korotyaeva, M.E. Stochastic excitation method for calculating the resolvent band structure of periodic media and waveguides. *Phys. Rev. B* **2018**, *97*, 224110. [CrossRef]